Case Studies in Engineering Failure Analysis 1 (2013) 120–130

Contents lists available at SciVerse ScienceDirect

Case Studies in Engineering Failure Analysis

journal homepage: www.elsevier.com/locate/csefa

Case study

Metallurgical analysis of SA-106 Gr. B pipe failure during hot bending

A.H.V. Pavan [a,*], K.S.N. Vikrant [a], G. Vimalan [b], Kulvir Singh [a]

[a] Metallurgy Department, BHEL, Corporate R&D Division, Vikasnagar, Hyderabad 500 093, India
[b] Welding Research Institute, BHEL, Tiruchirappalli 620 014, India

ARTICLE INFO

Article history:
Received 22 January 2013
Received in revised form 1 May 2013
Accepted 4 May 2013
Available online 21 May 2013

Keywords:
Circumferential crack
Hot-bending
SA-106 Gr. B steel
Dendritic morphology
Over-stress

ABSTRACT

This investigation deals with failure analysis of SA-106 Gr. B pipe which is a Carbon-Manganese steel used for moderately high temperature applications in industries. A transverse/ circumferential crack was formed in SA-106 Gr. B steel pipe during hot-bending operation. Visual examination and stereo-microscopic analysis indicated the presence of globules on the intrados surface of the pipe and towards the inner section on the crack surface. The globules had dendritic morphology which indicated the melting of the metal caused by temperature hike. Detailed analysis of the microstructure clearly indicated the presence of groups of inclusions. These inclusions coupled with over-stress due to sudden increase in temperature during induction heating led to the formation of cracks and caused failure of the pipe.

© 2013 Elsevier Ltd. Open access under CC BY-NC-ND license.

1. Introduction

SA-106 Gr. B is a carbon–manganese steel intended for various high temperature service applications such as feed-water reducers in Pressurized Water Reactors (PWR) [1], liquid ammonia transport from ammonia heater to urea reactor [2], drain lines in power reactor components [3], and feeders for carrying out the Primary Heat Transport (PHT) coolant to reactor core [4]. This material is prone to low cycle corrosion-fatigue [1], pitting corrosion [2], intergranular cracking and flow assisted corrosion (FAC) [4]. In context of fossil fired thermal power plants, SA-106 Gr. B material is used in low temperature regime components (such as ring feeder of the boiler and drain pipes from condenser to boiler feed water inlet) where water is the working medium and operating temperatures are between 80 and 120 °C. Ring-feeder is important in order to deliver water which will be uniformly heated through various tubes passing through the furnace wall to the boiler drum. Drain pipes handle condensed water from hot-well of the condenser to the boiler feed-water inlet, for a distance of the order of hundreds of meters. They also have bends which have to be pre-fabricated before assembly at the site. Hot bending operation is hence employed to bend the pipes as per the required specifications of a particular unit.

The schematic of hot bending is indicated in Fig. 1. This process involves a pipe fixed at two ends with clamps and an induction heating coil placed at the region where the pipe is supposed to be bent. One clamp moves towards the induction coil at a constant speed while the other clamp rotates as per the desired, preset parameters and also moves at the same speed of the other clamp simultaneously, thereby bending the heated portion of the pipe.

* Corresponding author. Tel.: +91 970 198 5279; fax: +91 40 2377 320.
E-mail addresses: pavanahv@bhelrnd.co.in, pavanahv@gmail.com (A.H.V. Pavan).

2213-2902 © 2013 Elsevier Ltd. Open access under CC BY-NC-ND license.
http://dx.doi.org/10.1016/j.csefa.2013.05.001

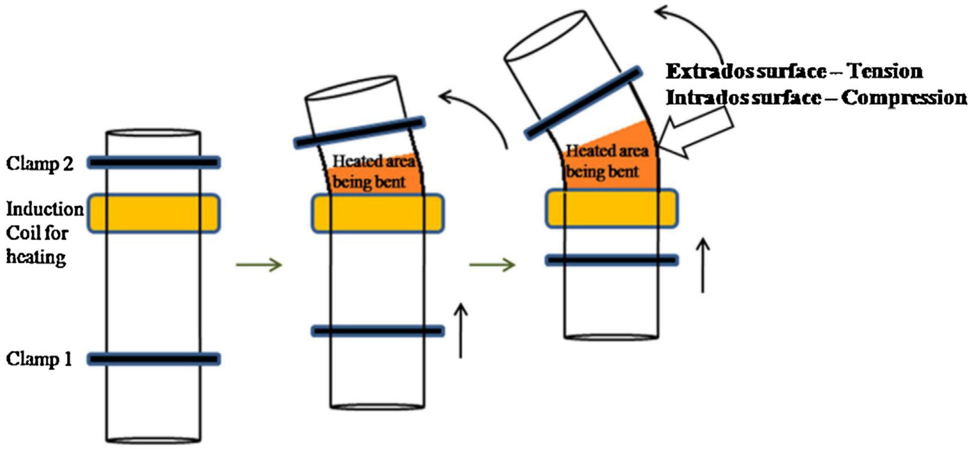

Fig. 1. Schematic of hot bending process adopted for bending SA-106 Gr. B pipe.

During hot bending operation at the shop floor, one of the pipes undergoing bending operation developed a large circumferential/transverse crack. The pipe is made of SA-106 Gr. B steel as per the ASME specifications [5]. The initial dimensions of the pipe were ∅ 508 mm × 30 mm and the hot bending temperature was 900–950 °C. The thickness and bend angle of the pipe to be achieved were 15 mm and 45° respectively. The failure occurred when the pipe was being bent by 4–5° only. Due to this unexpected failure, the pipe was removed from the bending equipment and a failure analysis was proposed to be conducted. A small portion of the pipe as indicated in Fig. 2(b) was cut and sent for failure investigation. This pipe will be referred to as "failed pipe" in this investigation. Also, a portion of another pipe which did not show any failure after hot bending was also provided to compare the properties of both the pipes. This pipe will be referred to as "good pipe" in this investigation.

The following procedure was adopted to understand the failure of the pipe during hot bending:

1. Visual examination and stereomicroscopy of the as-received pipe sample, both on the intrados and extrados surfaces as well as the surface of the crack.
2. Chemical analysis of both the good pipe as well as the failed pipe materials.
3. Metallography and microstructural examination of both the good pipe as well as the failed pipe materials.
4. Hardness measurements.
5. Mechanical testing to reveal mechanical properties such as tensile strength at various temperatures, impact strength at room temperature and % reduction in area.
6. Fractography of the failed surfaces after ultrasonic cleaning.

2. Experimentation

A portion of the failed pipe was sent for failure investigation after cutting it carefully at the site and packing it without damaging the surface features. The as-received portion of the pipe for failure investigation is shown in Fig. 2. After visual examination and stereomicroscopy of the extrados and intrados surfaces, the specimen was intentionally broken in liquid nitrogen to reveal the surface of the crack across the pipe wall. Stereomicroscopic studies were conducted using Leica Z6 APO stereomicroscope. Fractography on the specimen was carried out using Zeiss Supra 55 VP Field Emission Scanning Electron Microscope (FESEM) and compatible Energy Dispersive X-ray Spectroscopy (EDS) equipment from Oxford Instruments. Subsequent to fractography of the surface of the crack, sampling was carried out to prepare specimen for microstructural examination from the heat affected zone of the pipe and for evaluation of chemical and mechanical properties from the un-affected portion of the pipes respectively.

Chemical composition was obtained using Spectromax X, Optical Emission Spectrometer (OES), after grinding the sample as per the sample preparation specifications. For microstructural examination, the samples were ground with a series of emery papers and were polished with suspended particulate solutions subsequently from 9 μm to 0.25 μm and later with 0.05 μm alumina suspension. Etching was carried out on these specimens using 2% Nital solution. Microstructural examination was carried out using both optical microscopy and FESEM techniques. Optical microscopic studies were conducted using Leica DMI 5000M inverted metallurgical microscope.

Hot tensile testing was carried out in Gleeble 3500 thermo-mechanical simulator with heating rate of 40 °C s^{-1}, soaking time of 120 s and vacuum of 5×10^{-5} Torr was maintained for the entire duration of the test. ASTM E-8M standard [6] with a gauge diameter of 10 mm was used for preparing specimens for hot tensile testing. Impact testing was carried out on TINIUS OLSEN, USA make V-notch Charpy impact specimens prepared as per specifications in ASTM E23 standard [7]. Hardness testing was carried out on Shimadzu-HSV-30 Hardness tester with 1 kg load for test duration of 15 s. In order to understand

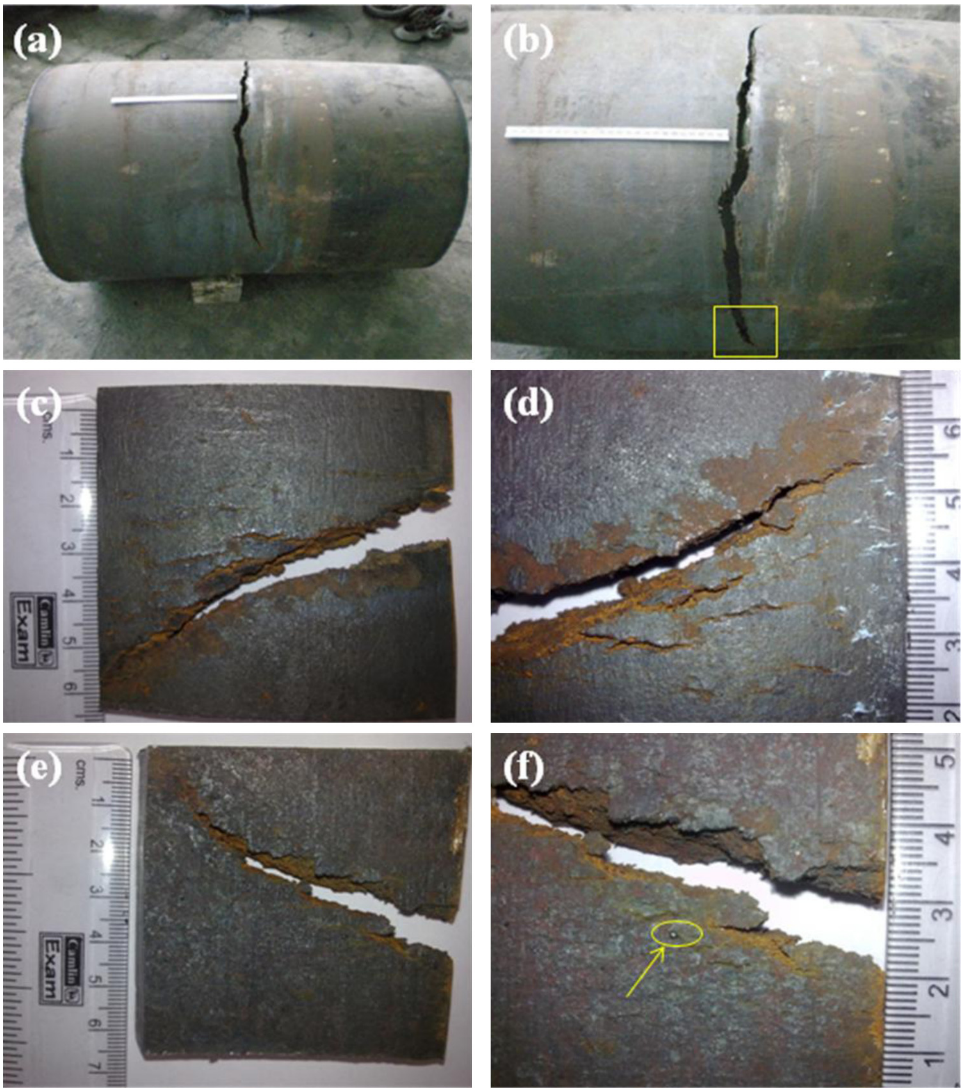

Fig. 2. (a) Actual pipe after removing it from the hot bending machine, (b) pipe indicating the portion cut for further investigations, (c and d) outer surface and (e and f) inner surface of the portion indicating the presence of globules on the surface.

the failed pipe specimens' properties deviation from the standards, good pipe material was taken and same testing procedures were adopted in order to compare the results with those of the failed pipe.

3. Results

3.1. Visual examination

The pipe which had failed was inspected and a large transverse/circumferential crack was observed. A small portion towards an end of the crack (Fig. 2(b)) was cut and observed with naked eye. The extrados and intrados surfaces had an oxide scale over it with branching of fine cracks. In addition to these observations, the intrados surface had a number of globules over it (a large globule is indicated in Fig. 2(f)), all of which had metallic appearance. Similar kinds of globules were observed on the crack surface towards the intrados surface. In case of good pipe, there was only oxide scale which was observed over the surfaces of the pipe after hot bending operation.

3.2. Stereomicroscopy

Stereomicroscopy was carried out on the sampled failed pipe portion was cut in order to understand in detail, the features present on the inner surface of the tube and fracture surface. A thick and tenacious oxide scale was observed close to the

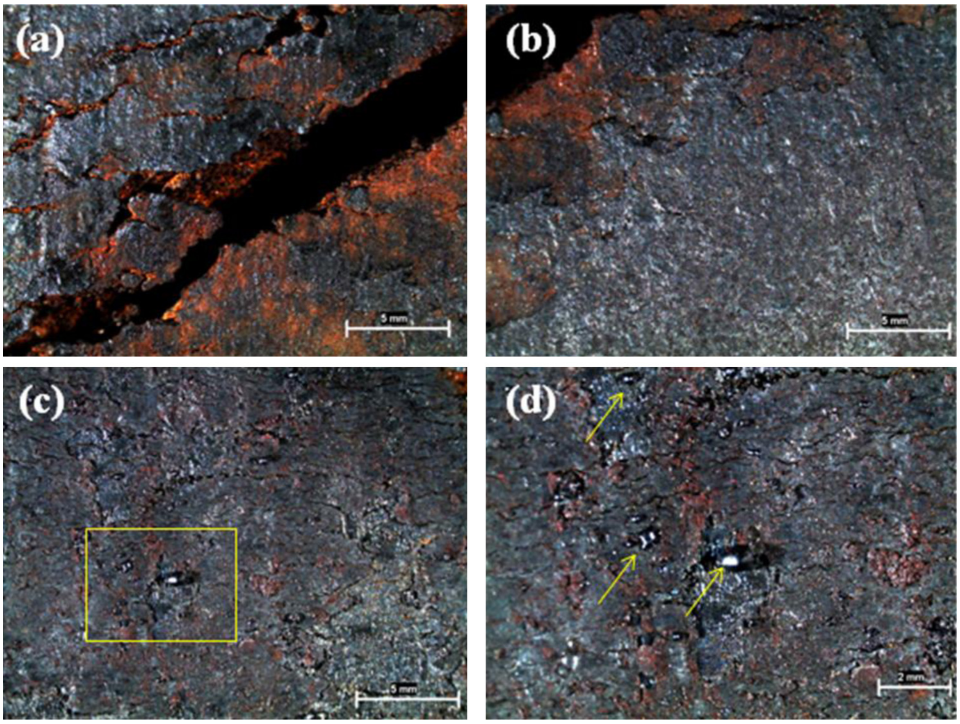

Fig. 3. (a and b) Outer surface of the pipe indicating thick oxide scale, (c and d) inner surface of the pipe indicating the presence of globules having metallic appearance and (d) magnified view of the region indicated in (c).

crack on the extrados surface while the intrados surface clearly indicated the presence of globules having metallic appearance (Figs. 3 and 4). These globules had formed on the inner surface of the crack as well as over the interior surface of the pipe (Fig. 5).

3.3. Microstructural characterization

Optical microscopic and FESEM studies of the good pipe and the failed pipe specimens were conducted. There was change in microstructure of the pipe from ferrite–pearlite (Figs. 6(a) and 7(a)) in case of good pipe specimen to Widmanstätten ferrite–pearlite (Figs. 6(b) and 7(b)) kind of morphology in case of failed pipe specimen. Cracks were also observed in the latter microstructure. Electron micrographs also indicate the presence of groups of inclusions (Fig. 8). The inclusions were identified as Sulfides having distinct regions one rich in Al while the other rich in Mn (Fig. 9).

3.4. Chemical analysis

Chemical analysis results of failed pipe and good pipe along with nominal composition of SA-106 Gr. B pipe are indicated in Table 1. The presence of small amounts of Al, Bi, Sn and As in the failed pipe was observed.

3.5. Fractography

Fractography was carried out on the surface of the crack towards the interior edge especially on the globules present. Dendritic morphology was clearly observed on the surface of these globules (Fig. 10(c) and (f)). These observations indicated that there has been melting and solidification of liquid metal. EDS analysis on these globules clearly indicates that the qualitative chemical composition of these are similar to the base metal as obtained during microstructural examination. In addition to the existing results, it was observed that the base of these globules which was attached to the surface of the crack contained Al, Si in significant quantities (as shown in Fig. 11, spot 1 and Table 2). The portion which was observed to be non-conducting in Fig. 10(c) was due to the fact that the sample was cleaned in acetone and it led to the formation of a layer rich in carbon.

3.6. Mechanical testing

Bulk hardness testing was carried out on polished specimen taken from both failed pipe as well as that of good pipe. About 20 indents were taken on each of the specimen. The results as indicated in Table 3 suggest that the hardness of failed pipe

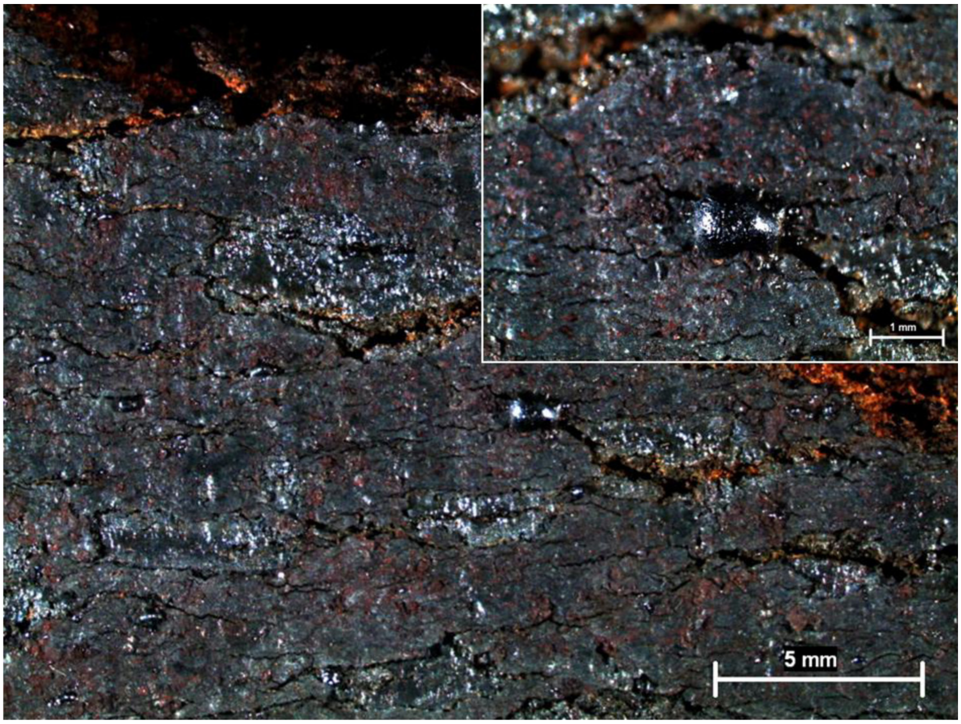

Fig. 4. Inner surface close to the crack indicating globules (inset: higher magnification of the globule).

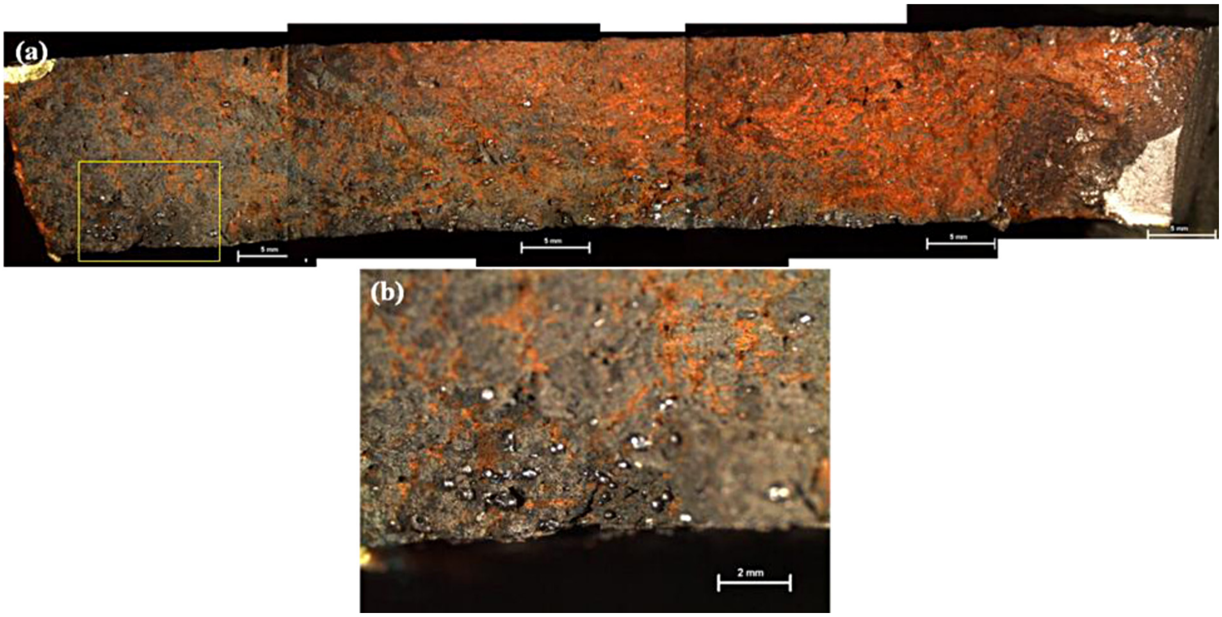

Fig. 5. Stereomicroscopic images of surface of the crack. (a) Fractured surface of the pipe clearly indicating the presence of globules towards the inner side of the pipe and (b) magnified view of the globules.

material was higher than that of the good pipe material. This was complementing the fact that Widmanstätten ferrite was observed due to the higher hardness.

Impact testing by Charpy method was carried out on the specimens prepared from failed pipe material as well as good pipe material. The results (as indicated in Table 3) clearly show that the impact strength (toughness) of failed pipe specimen was significantly low leading to lesser reduction in area as compared to that of the good pipe specimen which was reflected in the stereomicroscopy images of the respective impact specimen (Fig. 12).

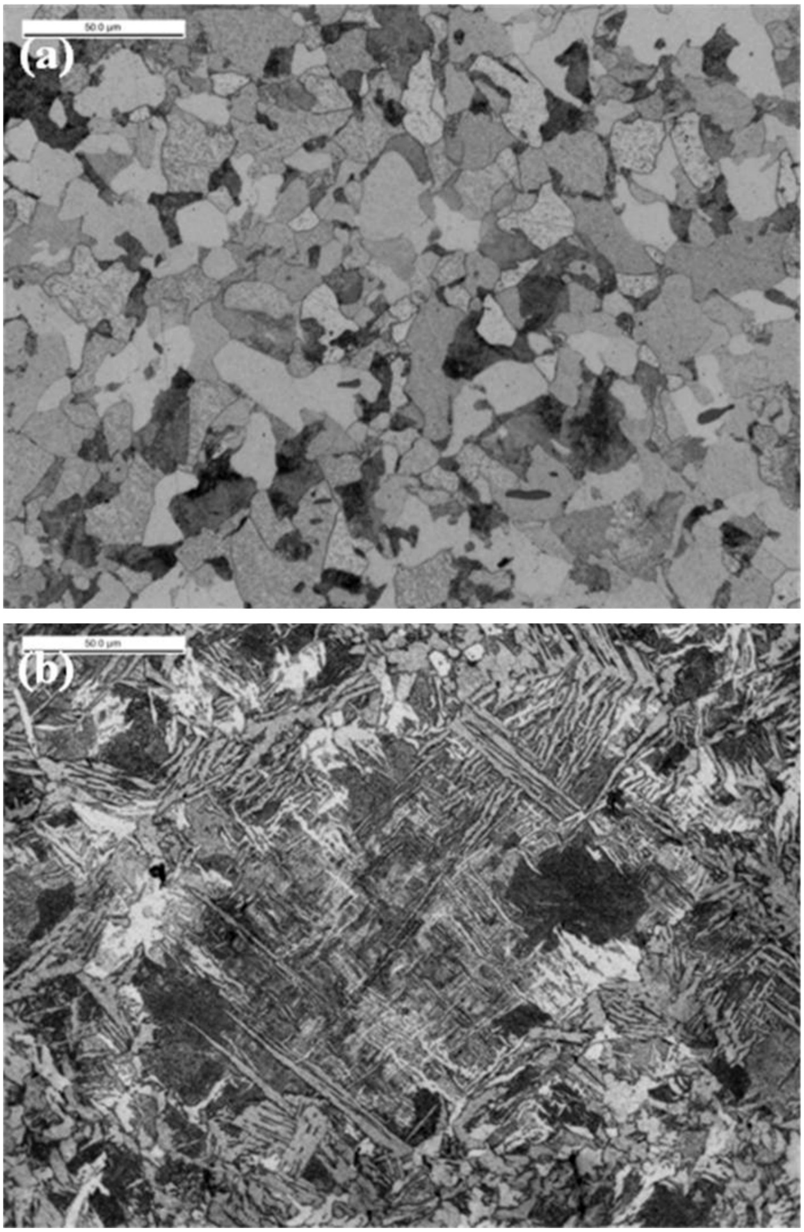

Fig. 6. Optical micrographs of (a) good SA-106 Gr. B sample and (b) failed pipe.

Hot tensile testing results (Table 4) indicated that the tensile strength of both the materials at various temperatures was similar. The reduction in area was significantly lower for the failed pipe specimens compared with the good pipe material specimens. This was also in trend with the impact testing values which led to similar conclusion on the toughness of the material.

4. Discussion

SA-106 Gr. B is a plain carbon steel. Plain carbon steels oxidize and form a thick oxide layer when they are heated to higher (beyond red-hot) temperatures. Therefore, the thick oxide scales observed on the extrados and the intrados surfaces formed when the pipe was heated to 900–950 °C in air by induction heating during hot bending.

Visual inspection and stereomicroscopic studies clearly indicated the presence of the globules on the intrados surface. Also, stereomicroscopic studies of the surface of the crack revealed the presence of similar kinds of globules on the surface towards the intrados surface. Fractography of these globules indicated presence of distinct dendritic morphology over their surface. EDS results on the surface of these globules indicated composition similar to that of base metal while base of these

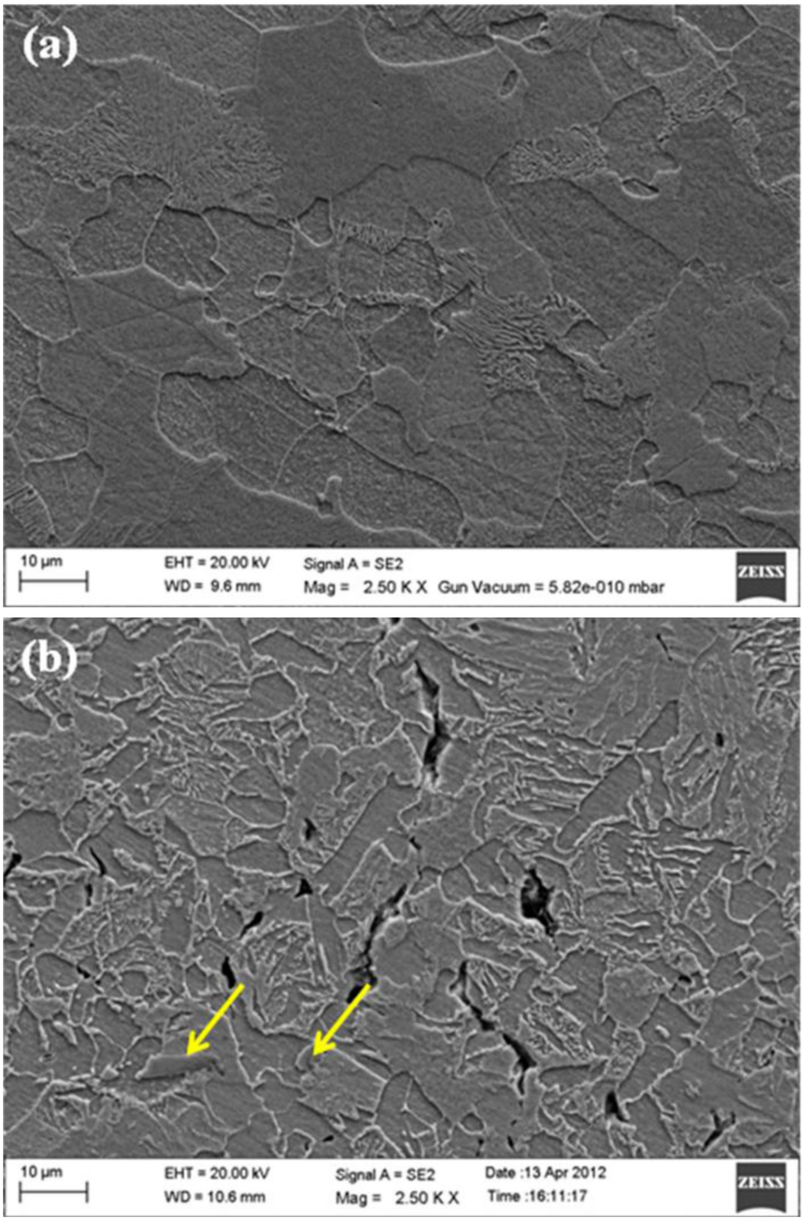

Fig. 7. Electron micrographs of (a) good SA-106 Gr. B sample and (b) failed pipe indicating MnS inclusions.

globules had higher Al, Si content. This confirmed melting and solidification of the base metal suggesting that higher temperature was attained during operation. Also, optical micrographs indicated the presence of Widmanstätten ferrite–pearlite in the failed pipe which was complimented by higher hardness results. This morphology of ferrite appears when there is sudden increase of temperature followed by moderate cooling rate.

From the electron micrographs, presence of groups of inclusions was observed. The presence of these inclusions led to significantly lower ductility and impact toughness of the failed material which could have bolstered the crack formation. This explains the presence of cracks originating from the inclusions due to excessive deformation during bending process. This may have occurred by sudden thermal expansion of pipe during induction heating of the pipe.

The intrados and extrados surfaces of the pipe located away from the bend angle, experience compressive and tensile stresses, respectively during bending as indicated in Fig. 1. Therefore, the temperature hike which led to localized melting of base metal, seeped out through the cracks developed from the inclusions, into the intrados surface due to compressive stress, thus, forming metallic globules.

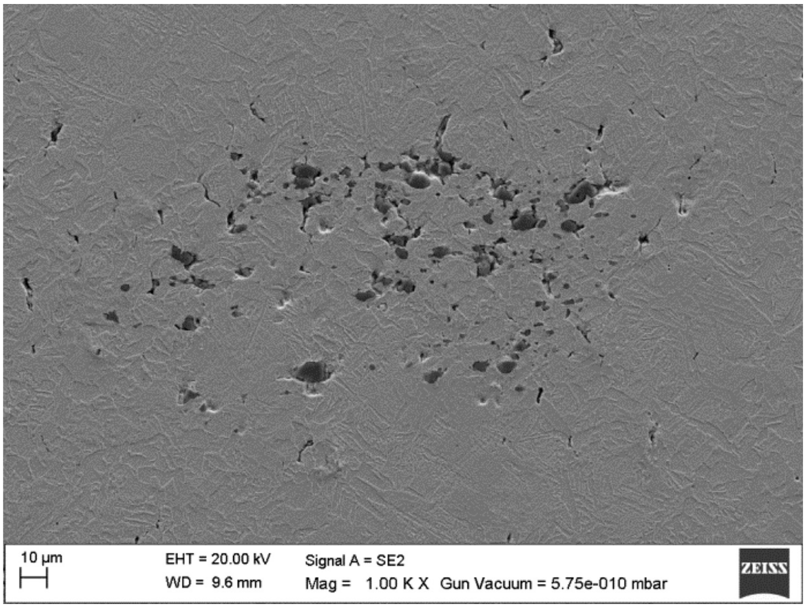

Fig. 8. Groups of inclusions observed in the failed pipe.

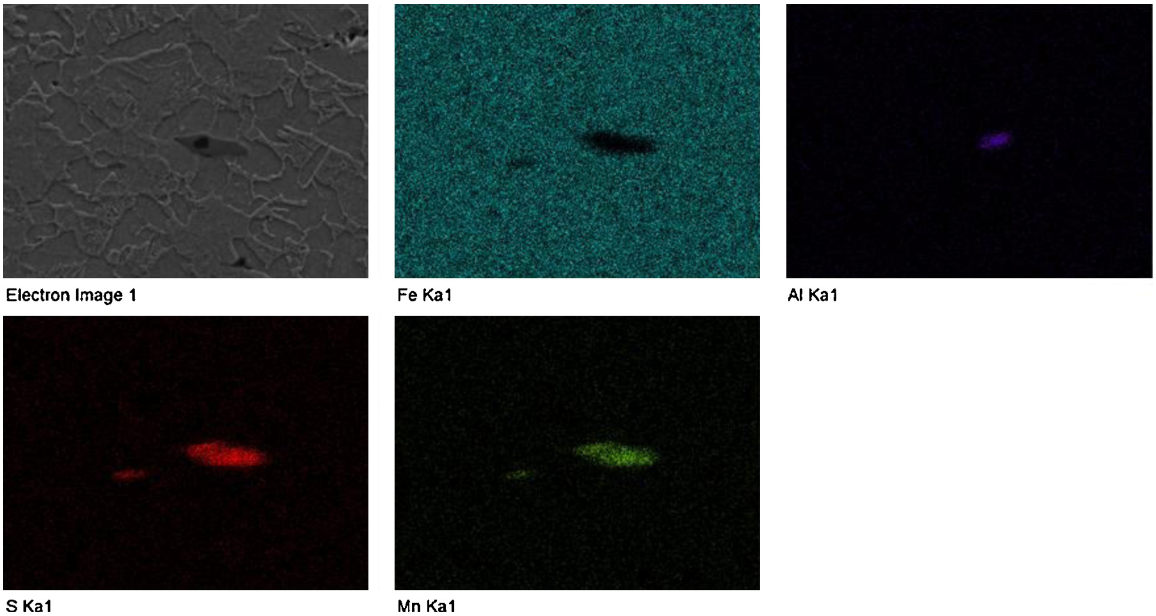

Fig. 9. Elemental mapping of the inclusion revealed the sulfide inclusion indicating distinct regions rich in Al and Mn.

Table 1
Chemical composition results.

SA-106 Gr. B	C	Mn	P	S	Si	Cr	Cu	Mo	Ni	V	Others
Nominal[a] [7]	0.30 max	0.29–1.06	0.035 max	0.035 max	0.1 min	0.4 max	0.4 max	0.15 max	0.4 max	0.08 max	
Failed pipe	0.23	0.7	0.012	0.025	0.35	0.09	0.01	0.01	0.05	Trace	Al: 0.05; Bi, Sn, As: 0.01; W < 0.01; Pb, Zn, Sb-trace
Good pipe	0.23	1.10	0.021	0.025	0.28	0.15	0.11	–	0.06	–	Al: 0.02; Nb-traces

[a] For each reduction of C by 0.01% below specified max, an increase in Mn of 0.06% above the specified max will be permitted upto a maximum of 1.35%; Cr + Cu + Mo + Ni + V should not exceed 1%.

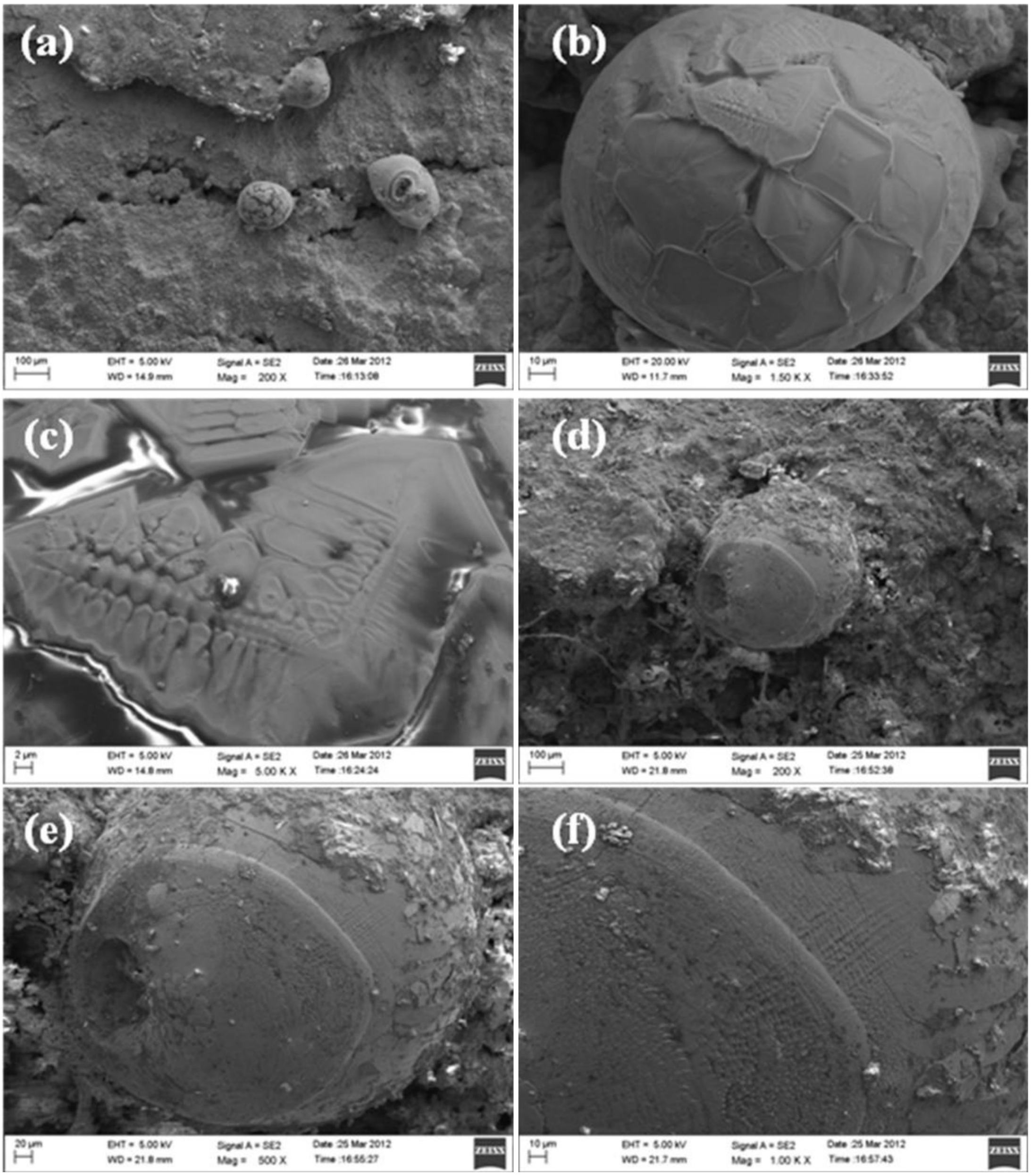

Fig. 10. (a and b) Fractographs clearly indicating the presence of globules on the surface of the crack, (c) higher magnification fractograph clearly depicting dendritic structure and (d–f) fractographs indicating another yet similar metal-like globule.

Table 2
EDS results (in wt.%) of the spots as shown in Fig. 11.

Spot/element	K	O	Al	Si	Ca	Ti	Fe	C	Mn	S	Cl	Na	Mg
Spot 1	0.67	50.78	1.50	3.68	1.08	–	23.22	19.05	–	–	–	–	–
Spot 2	–	35.34	–	–	–	–	50.95	13.26	0.45	–	–	–	–
Spot 3	–	35.57	–	–	–	–	50.59	13.35	0.49	–	–	–	–
Spot 4	0.17	38.35	0.88	1.40	0.95	0.44	41.49	14.41	0.40	0.74	0.20	0.56	–
Spot 5	–	35.02	–	–	–	–	51.37	13.14	0.46	–	–	–	–
Spot 6	–	45.09	–	–	–	–	37.69	16.92	0.30	–	–	–	–
Spot 7	1.03	37.84	2.39	5.06	2.73	0.39	30.64	14.35	–	1.78	1.76	1.28	0.74
Spot 8	0.67	50.78	1.50	3.68	1.08	–	23.22	19.05	–	–	–	–	–

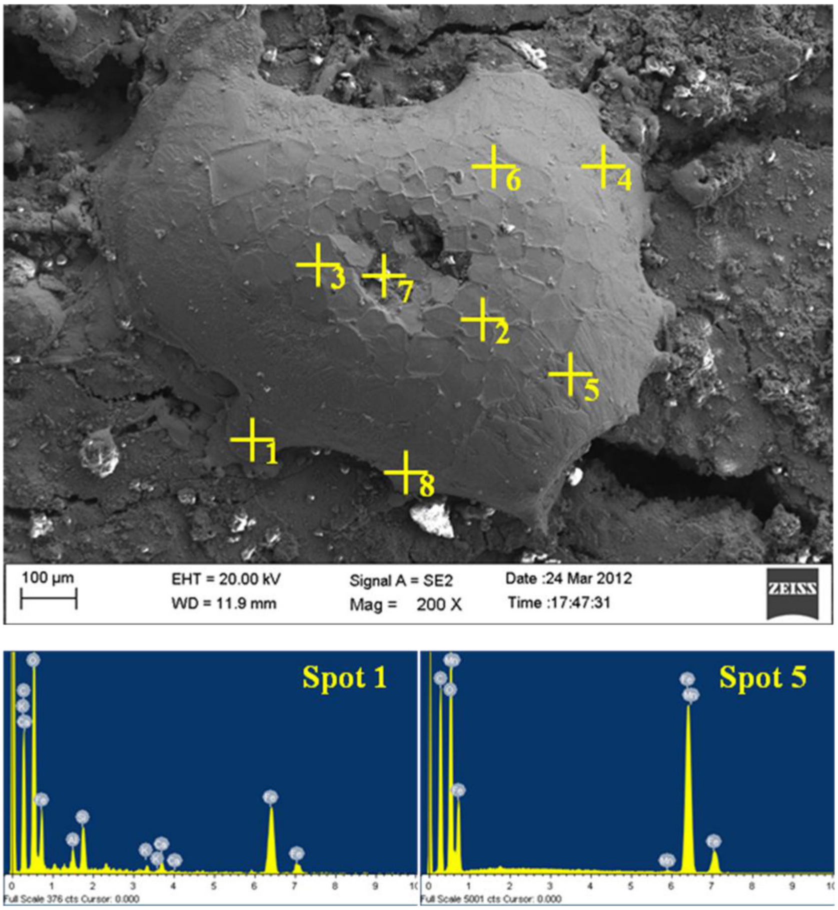

Fig. 11. EDS spots on the micrograph and their respective spectra on a globule.

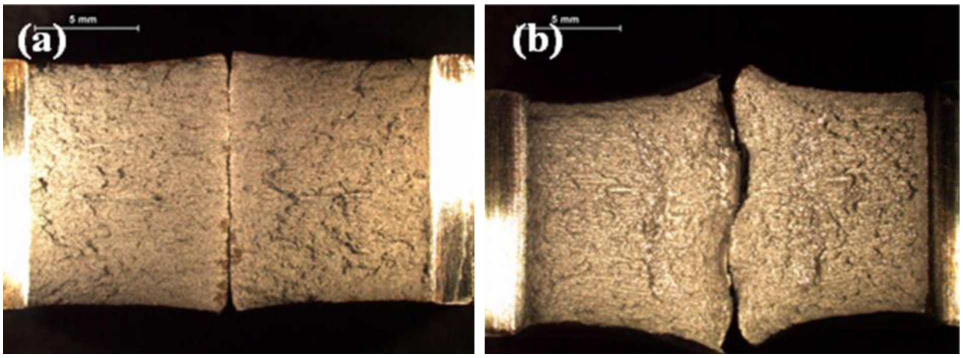

Fig. 12. Stereomicrographs of (a) failed pipe and (b) good pipe impact specimen.

Table 3
Hardness results of good pipe and the failed pipe.

Sample	Mean hardness (HV_1)	Impact strength (J)
Failed pipe	225 ± 19	39
Good pipe	151 ± 7	112

Table 4
Hot tensile testing results of failed pipe and good pipe specimen.

Sample	Temperature (°C)	UTS (MPa)	% Reduction in area
Failed pipe material	800	110.88	46.71
	850	105.03	51.28
	900	87.37	40.71
	950	72.17	35.04
	1000	61.64	39.47
Good pipe material	800	109.68	60.31
	850	105.78	78.84
	900	84.13	81.85
	950	68.33	92.92
	1000	57.83	95.42

5. Conclusions

It can be concluded the failure of the pipe during hot bending operation was due to simultaneous temperature over-shoot and the formation of cracks at inclusion sites due to the bending stresses and over-stress resulting from sudden thermal expansion during induction heating process. The metal in the localized region of the cracks which originated at the regions having groups of inclusions had undergone melting as a result of temperature hike. This led to the formation of metallic globules when the metal seeped out through the cracks in liquid condition due to compression stress acting on the intrados surface during bending.

This could possibly be avoided by stringent quality control of the pipe material for pipes as well as maintaining the operation parameters within the limits during hot bending process.

Acknowledgements

Authors express their gratitude to the management of BHEL for financially supporting this study. They appreciate the encouragement, motivation and support extended by Shri. H. Krishnan, General Manager (MDM & P) (Retired). They acknowledge Shri. S. Manimozhi, Sr. Deputy General Manager, and other concerned officials at Welding Research Institute (WRI) Trichy, for providing the samples and also arranging for hot tensile tests on Gleeble. The help rendered by Shri. K. Satyanarayana, Executive Additional Engineer II, for stereomicroscopy is gratefully acknowledged.

References

[1] Czajkowski CJ. Cracking in a reducing pipe from a pressurized water reactor; pipes and pipelines. Handbook of case histories in failure analysis, vol. 2. Materials Park, OH, USA: ASM International; 1993. p. 163–7.
[2] Sivaprasad S, Narang SK, Singh R. Failure of high pressure ammonia line in a fertilizer plant – a case study. Engineering Failure Analysis 2006;13:867–75.
[3] Chavez SA, Korth GE, Harper DM, Walker TJ. High-temperature tensile and creep data for Inconel 600, 304 stainless steel and SA106B carbon steel. Nuclear Engineering and Design 1994;148:351–63.
[4] Slade JP, Gendron TS. Flow accelerated corrosion and cracking of carbon steel piping in primary water – operating experience at the Point Lepreau Generating Station. In: Proceedings of the 12th international conference on environmental degradation of materials in nuclear power system – water reactors. Warrendale, Pennsylvania: TMS (The Minerals, Metals and Materials Society); 2005. p. 773–84.
[5] ASME boiler and pressure vessel code: II part A, ferrous material specifications (beginning to SA-450) materials. Three Park Avenue, NY, USA: ASME Boiler and Pressure Vessel Committee on Materials; 2010. p. 195–205.
[6] ASTM E8/E8M-09. Standard test methods for tension testing of metallic materials. In: American Association State Highway and Transportation Officials Standard, AASHTO no.: T68, an American national standard. West Conshohocken, PA, USA: ASTM International; 2009. p. 1–27.
[7] ASTM E23-07a. Standard test methods for notched bar impact testing of metallic materials, an American national standard. ASTM International: West Conshohocken, PA, USA; 2007. p. 1–28.